Development of an Automatic Block Generation Algorithm

Final Report
NASA Joint Interchange NCC2-5099

by

Scott Eberhardt, Associate Professor
Byoungsoo Kim, Research Associate
Department of Aeronautics and Astronautics
University of Washington
Seattle, WA 98195

Absract

A method for automatic multi-block grid generation, developed as part of NASA Ames/ University of Washington Joint Interchange NCC2-5099, is described. The method combines the Modified Advancing Front Method as a Predictor with an elliptic scheme as a corrector. It advances a collection of cells by one cell height in the outward direction using Modified Advancing Front Method, and then corrects newly-obtained cell positions by solving elliptic equations. This predictor-corrector type scheme is repeatedly applied until the field of interest is filled with hexahedral grid cells. Given the configuration surface grid, the scheme produces block layouts as well as grid cells with overall smoothness as its output. The method saves human-time and reduces the burden on the user in generating grids for general 3-D configurations. It is used to generate multi-block grids for wings in their high-lift configuration.

INTRODUCTION

Grid generation is an essential and critical task for successful application of CFD in engineering process. Grid generation has been, and still is, a labor-intensive and expertise-requiring task, especially for complicated configurations. Configurations for which grid generation requires enormous amount of human-time and labor can be easily found: Automobiles, underwater vehicles, and airplanes. One example of further complication is that modern flying vehicles use high-lift devices, such as slats and multiple flaps, during take-off and landing. Flow fields around such complicated configurations are generally decomposed into several relatively-simple sub-domains. Once sub-domains are identified, it is relatively simple and straightforward to fill each of them with structured meshes.

A sub-domain may either share a common interface with immediately adjacent sub-domains or be overlaid with each other. The first strategy of using sub-domains with common interfaces is the subject of this research, and is called a multi-block grid approach. Decomposition of physical flow fields into blocks, so-called block generation, is the most challenging task in the process of multi-block grid generation. Development of an automatic block generation algorithm is one of several highly-pursued topics in the field of grid generation. (ref. 1 to 11). Many of existing block generation schemes generate block boundaries in their topological form. In other words, once the user is given those block boundaries, he/she should distribute grid points along those block boundaries and generate internal grid points for each block to obtain final multi-block grids.

In this report, the refinement of a new approach for automatic multi-block grid generation is presented. The new approach generates multi-block grids in a single step, instead of generating block boundaries first and then filling each block with a certain number of grid points specified by the user later. For realization of this unique feature, the user provides configuration surface grids and the grid spacing in the advancing direction as input to the scheme. These user-specified surface grids are undoubtedly composed of several blocks, especially for complicated configurations. This speculation is based on not only the fact that it is very difficult and undesirable to discretize a complicated configuration surface with a single structured grid but also the fact that the surface is likely to be described as a collection of relatively-simple segments. These segments may be created by geometry definition programs or CAD programs and the user may have, according to the expected flow phenomena, a preference on the grid point distribution along the surface, which is more easily accomplished by the use of multi-block surface grid. These user-specified surface grids will be the actual grid points along the block boundaries in the resulting multi-block volume grids, and play an active role in generating final grids as explained in the following section.

The method and results shown in this report have been presented in a conference paper (ref. 12).

METHOD

The method uses the combination of the Modified Advancing Front Method as a Predictor with an elliptic scheme as a corrector (MAP scheme). Kim introduced the MAP scheme for 2-D and used it for multi-block grid generation around 2-D configurations (ref. 13). The MAP scheme advances a collection of surface grid blocks by one cell height at a time. In this method, the collection of surface blocks which advances simultaneously is called a "front".

MAP scheme

As the name implies, the MAP scheme (an acronym of the Modified Advancing Front Method as a Predictor with an elliptic scheme as a corrector) is a predictor-corrector approach. A front is advanced by the predictor and smoothed by the corrector. Each front goes through this predictor-corrector step until the flow field of interest is filled with multi-block grids.

Predictor step.-It advances a front using the Modified Advancing Front Method. The Advancing Front Method (AFM) was originally developed for unstructured triangular meshes (ref. 14 to 16). In the present research, however, this method has been modified for hexahedral mesh generation. The Modified AFM not only enables simultaneous generation of a collection of hexaheral cells but also adjusts the distance and direction of advancement of each grid point according to the surrounding situation. It first interpolates the distance and direction of advancement for each internal point of a front from those values along the boundary of the front. Then, all the points on the front are advanced, resulting in a new front, and the same number of hexahedral cells as that of quadrilateral cells along the old front are obtained. In providing a surface grid as initial fronts, (i,j) indexing of each surface block should be ordered in a consistent manner so that its outward direction can be readily identified; e.g. right-handed rule to have the third k-axis as the outward direction, $\grave{e}_i \times \grave{e}_j \propto \grave{e}_k$. The new front, however, usually carries the non-smoothness, if any, of the old front, and magnifies it, making further advancement impossible or meaningless, especially for concave regions. This situation is avoided by adopting a corrector step.

Corrector step.-In the corrector step, Laplace's equations are used as the elliptic equations by following Cordova's approach (ref. 17). To apply the elliptic corrector, an image of the old front with respect to the new front is first introduced. Using these 3 fronts, 3-D Laplace equations are solved along the new front with the other two as fixed boundary conditions. This procedure is illustrated in Fig. 1. In this example, the initial front is composed of 3 blocks of surface grid, as shown in Fig. 1(a). The predicted front by the Modified AFM is shown in Fig. 1(b). The image front and the resultant 3-front system are shown in (c) and (d) of Fig. 1, respectively. As a solution to the elliptic equations, a smoother distribution of grid points for the new front is obtained, as shown in Fig.1(f), compared to that of the predicted front, as reproduced in Fig. 1(e).

Advancement of fronts.-The distance and direction of advancement of each front is predecided by the user ("free advancement"), except for the fronts which have adjacent fronts aligned in the direction of their own advancement ("guided advancement"). If a front falls into the second category, the distance and direction of advancement are decided by the adjacent fronts. The user-specified surface blocks can be grouped into as many number of fronts as the user wants, and the way they are grouped affects the structure of final multi-block grids. Examples of different structures of final volume grids through different setting of initial fronts are demonstrated for a simple hexahedral body in Fig. 2, Fig. 3, and Fig. 4. In Fig. 2, the 6 block surface grid of the hexahedral body is taken as a single front. As a result, the MAP scheme produces a 6 block grid, which shows a very smooth distribution of grid points along the outer block boundaries. On the other hand, Fig. 3 shows a different block structure due to different arrangement of initial fronts. In this example, the body surface blocks are grouped into 2 fronts; one front with 5 blocks and the other with one block. The two fronts are shown separated in Fig. 3(a). The resultant volume grid has 10 blocks (Fig. 3(b)), and the outer block boundaries are shown in (c). Fig. 4 shows a 26 block grid for the same configuration. In this example, each of 6 surface blocks is taken as a front of its own. In the results presented in this paper, two adjacent blocks are connected in the "complete" sense. In other words, they share an exactly same interface as one of their block faces. Adoption of the "complete" inter-block connectivity makes the total number of blocks in the resulting volume grids higher than that with the "partial" connectivity.

Bridging of distant fronts

For multi-body configurations such as high-lift wings, two distant fronts can march toward each other. One example is shown in Fig. 5: One front from the main wing and the other from the flap advance toward each other. If this situation is not dealt with properly, the two fronts will pass each other and generate hexahedral cells in the region which is already occupied by other cells. If two fronts are found advancing toward each other and less than a specified distance away, then the scheme will "bridge" the two with a third front. To bridge two distant fronts, proper grid lines along each front, "bridging edges", are first identified (A-B and C-D in Fig. 5).

Once the bridging edges are obtained, they are used to form a 3-D surface grid surrounded by the bridging edges and additional edges connecting them (A-C and B-D). This newly-obtained surface grid is called a "bridging" front. In general, the pair of bridging edges have a different number of grid points with respect to each other. Fig. 6 shows bridging fronts of different structures due to the difference in the number of grid points along the bridging edges and along the edges connecting them. With the help of the "bridging" front, the two distant fronts which were to collide with each other are connected with each other, and the advancement of those fronts will be adjusted accordingly. The sequential advancement of fronts continues until the user-specified outer boundary is reached. The scheme groups hexahedral cells properly, resulting in a multi-block volume grid system with "complete" inter-block connectivity.

EXAMPLES

The first example is for a generic 3-D single-element wing. NACA 0012 airfoil is used as its wing section, except the round wing tips which are formed by rotating the wing section at the last spanwise station, resulting in a half body of revolution. Fig. 7(a) shows the user-specified wing surface grid together with a surface grid for the wake-plane. Due to its geometrical shape, it is natural and easy for the user to generate the surface grid for the wing-tip region in such a way that all the grid lines in the chordwise direction converge into a single point on each end of the half body of revolution. The user doesn't have to provide the wake-plane grid. By providing it as a part of input, however, he/she can be assured to have the grid point distribution along the wake the way he/she wants. As explained earlier, a "front" is supposed to advance in only one direction. This

means that the wake-plane grid is composed of two sets of exactly same grids glued to each other back to back. One set has a reversed ordering of index (i,j) with respect to that of the other. The initial surface grid is composed of 6 surface blocks with "complete" connectivity; one on the upper side of the wing, one on the lower side of the wing, two on both wing tips, one on the upper side of the wake-plane, and the last on the lower side of the wake-plane. By taking those 6 block surface grid as a single "front" and specifying the grid spacing in the advancing direction, the MAP scheme generates 6 block volume grid. The block edges of the resultant grid system are shown in Fig. 7(b). The block boundary grid lines along the symmetry plane are also included. Generating this grid system can be thought of as the analogy of blowing a balloon with the initial shape of Fig. 7(a). The outer block boundaries, shown in Fig. 7(c), and the internal block boundaries, shown in Fig. 7(d), indicate that the grid point distribution becomes smoother and more evenly-spaced as the front advances outward.

In the previous example, the block structure of the resulting volume grid is naturally decided by the block structure of the initial surface grid. With the MAP scheme, however, totally different block structures of volume grids can be easily obtained from the same initial surface grid by changing the arrangement of initial fronts, and it is demonstrated in the next example. Fig. 8(a) shows the exactly same surface grid as Fig. 7(a). In this example, the 6 block surface grid is divided into 3 fronts. One front has 4 surface blocks; the upper wing surface, the lower wing surface, the upper wake surface, and the lower wake surface. The other two fronts have one surface block from each wing tip. In this example, the two wake-plane blocks do not have connectivity at both spanwise ends. The MAP scheme generates a 14 block volume grid as an output. Fig. 8(b) shows the block edges. The outer block boundaries and the internal ones are shown in Fig. 8(c) and (d). These first two examples show the flexibility of the MAP scheme.

The next example is for a simplified high-lift configuration wing. Fig. 9(a) shows a 6 block configuration surface grid; 3 blocks on the main wing and 3 on the flap. The wing tip of the flap is flat while that of the main wing is round. The gap between the main wing and the flap is filled with a "bridging" front, as shown in Fig. 9(b). The resultant 28 block volume grid is shown in Fig. 9(c) and (d). In this example, the number of grid points along the leading edge of the flap is same as the number of points along the trailing edge of the wing. This situation is not always true. The present wing-flap configuration is a simplified and specific one, i.e. a full-length flap. One step toward generalization with the same configuration is to use a different number of grid points in the spanwise direction for the wing and the flap.

Fig. 10(a) shows the same configuration wing as Fig. 9(a). In this example, however, the flap has more grid points in the spanwise direction than the previous case. The "bridging" front should be formed in accordance to the number of grid points along the bridging edges, and the result is shown in Fig. 9(b). Once distant fronts are bridged with the help of a bridging front, the MAP scheme advances each front until the outer boundary is reached. Block edges and outer block boundaries of the resulting 38 block volume grid are shown in Fig. 9(c) and (d) respectively.

CONCLUSION

The MAP scheme can generate multi-block grids in an automatic fashion. As an input for the scheme the user provides a body surface grid and the grid spacing in the advancing direction. The user can choose how he/she wants to group the surface blocks to form initial fronts. The present scheme produces block layouts as well as grid cells of smooth distribution as its output. Due to its unique approach, the present method saves human-time and reduces the burden on the user in generating grids for general 3-D configurations. The configuration of the high-lift wings shown in this paper, however, is not general enough. Generalization and improvement of the grid generation program using the MAP scheme for realistic 3-D configurations is currently underway.

REFERENCES

1. Schonfeld, T., and Weinerfelt, P., "The Automatic Generation of Quadrilateral Multi-Block Grids by the Advancing Front Technique," Proceedings of the 3rd International Conference on Numerical Grid Generation in CFD, Barcelona, Spain, June 3-7, 1991.

2. Stewart, M.E.M., "Domain-Decomposition Algorithm Applied to Multielement Airfoil Grids," AIAA Journal, Vol. 30 No. 6, pp1457-1461, June, 1992.

3. Andrews, A.E., "Knowledge-Based Flow Field Zoning," *Numerical Grid Generation in Computational Fluid Mechanics '88*, Pineridge Press, pp 13-22, 1988.

4. Weatherill, N.P., and Shaw, J.A., "Component adaptive grid generation for aircraft configurations," AGARD-AG-309, pp 29-39, 1988

5. Shaw, J.A., Georgala, J.M., and Weatherrill, N.P., "The Construction of Component-Adaptive Grids for Aerodynamic Geometries," *Numerical Grid Generation in Computational Fluid Dynamics '88*, Pineridge Press, pp383-394, 1988

6. Georgala, J.M., and Shaw, J.A., "A Discussion on Issues Relating to Multiblock Grid Generation," AGARD-CP-464, 1990.

7. Allwright, S.E., "Techniques in Multiblock Domain Decomposition and Surface Grid Generation," *Numerical Grid Generation in Computational Fluid Dynamics '88*, Pineridge Press, pp 559-568, 1988

8. Allwright, S., "Multiblock Topology Specification and Grid Generation for Complete Aircraft Configurations," AGARD-CP-464, 1990.

9. Dannenhoffer, J.F. III, "A Block-Structuring Technique for General Geometries," AIAA 91-0145, Reno, January 1991.

10. Dannenhoffer, J.F. III, "A New Method for Creating Grid Abstractions for Complex Configurations," AIAA 93-0428, Reno, January 1993

11. Noble, S.S., and Cordova, J.Q., "Blocking Algorithms for Structured Mesh Generation," AIAA92-0659, 1992

12. Kim, B., and Eberhardt, S. "Automatic Multi-Block Grid Generation for High-Lift Configuration Wings," NASA CP-3291, NASA Workshop on Surface Modeling, Grid Generation, and Related Issues in CFD Solutions, Cleveland, Ohio, May, 1995

13. Kim, B., Automatic Multi-Block Grid Generation about Complex Geometries, PhD. Dissertation, University of Washington, 1994

14. Lo, S.H., "A New Mesh Generation Scheme for Arbitrary Planar Domains," Int. J. Num. Meth. Eng., Vol. 21, pp.1403-1426, 1985.

15. Peraire, J. et al, "Adaptive Remeshing for Compressible Flow Computations," J. Comp. Phys. 72, PP.449-466, 1987.

16. Lohner, R., and Parikh, P., "Generation of Three-Dimensional Unstructured Grids by the Advancing Front Method," AIAA Paper 88-0515, Reno, January 1988.

17. Cordova, J.Q.,"Advances in Hyperbolic Grid Generation," 4th International Symposium on Computational Fluid Dynamics, Davis, CA, Sep. 1991

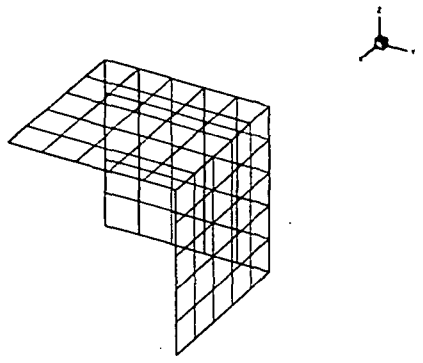

(a) The old front

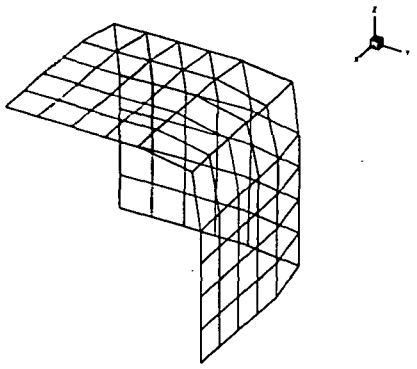

(b) The predicted new front

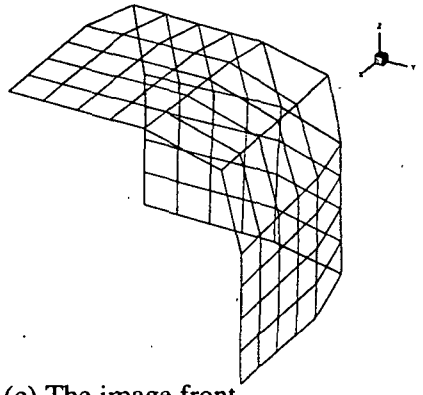

(c) The image front

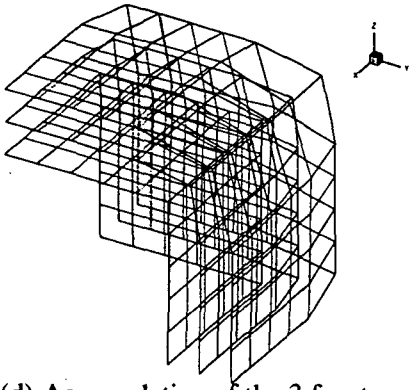

(d) Accumulation of the 3 fronts

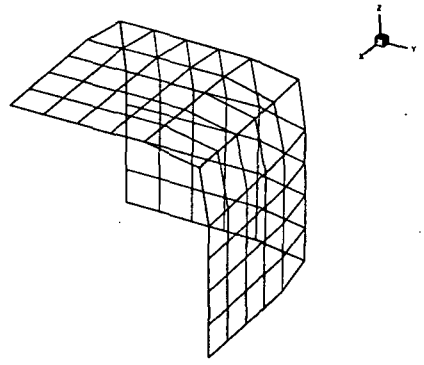

(e) The predicted new front, (b)

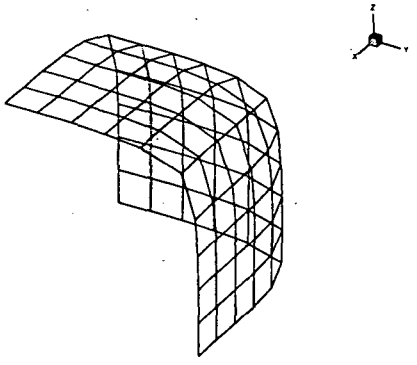

(f) The corrected new front

Fig. 1 Procedure of the predictor-corrector approach

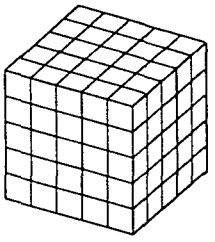

(a) Initial front with 6 block surface grid

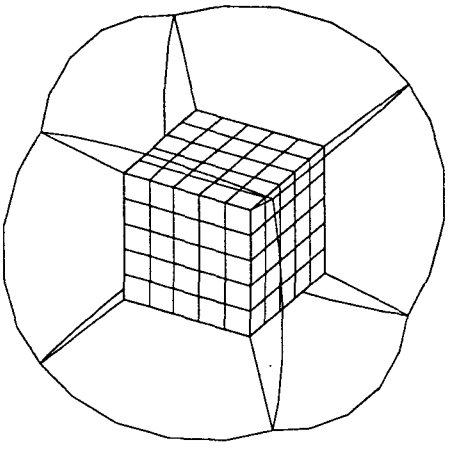

(b) Block edges of the resulting 6 block volume grid

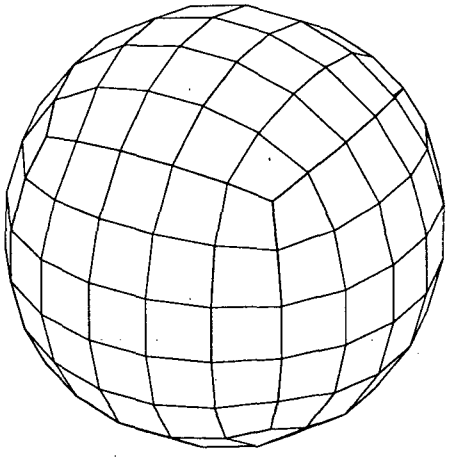

(c) Outer block boundaries

Fig. 2 6 block volume grid generation about a hexahedral body

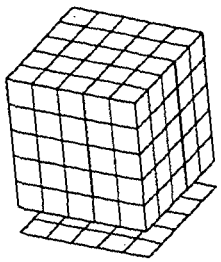

(a) 2 initial fronts: One with 5 surface blocks and the other with 1 block

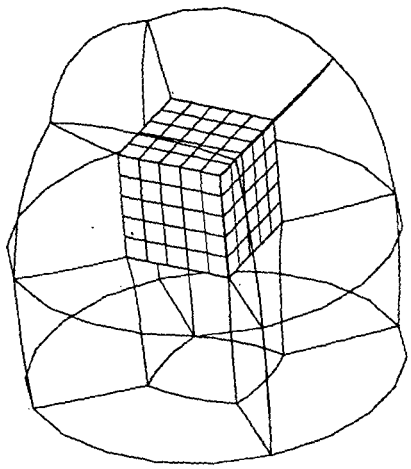

(b) Block edges of the resulting 10 block volume grid

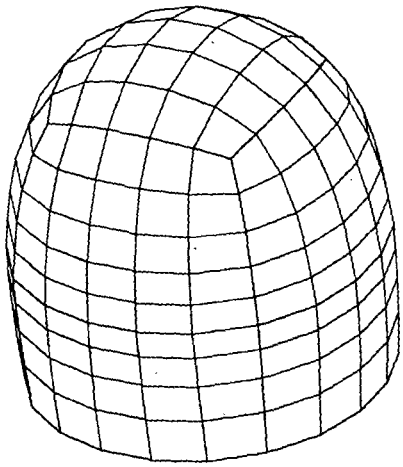

(c) Outer block boundaries

Fig. 3 10 block volume grid generation about a hexahedral body

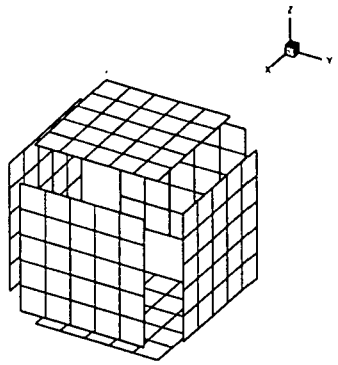

(a) 6 initial fronts: Each with 1 surface block from each face

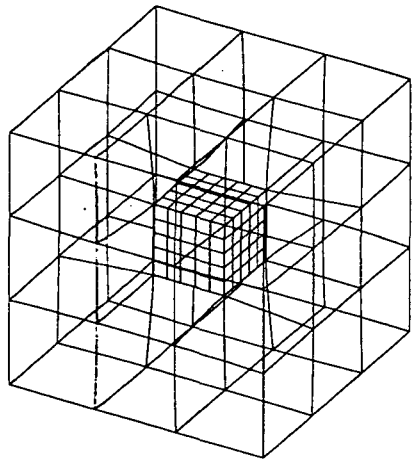

(b) Block edges of the resulting 26 block volume grid

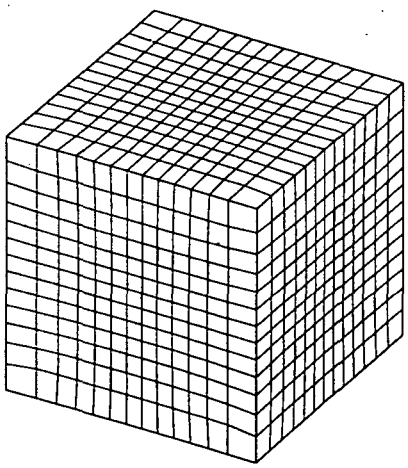

(c) Outer block boundaries

Fig. 4 26 block volume grid generation about a hexahedral body

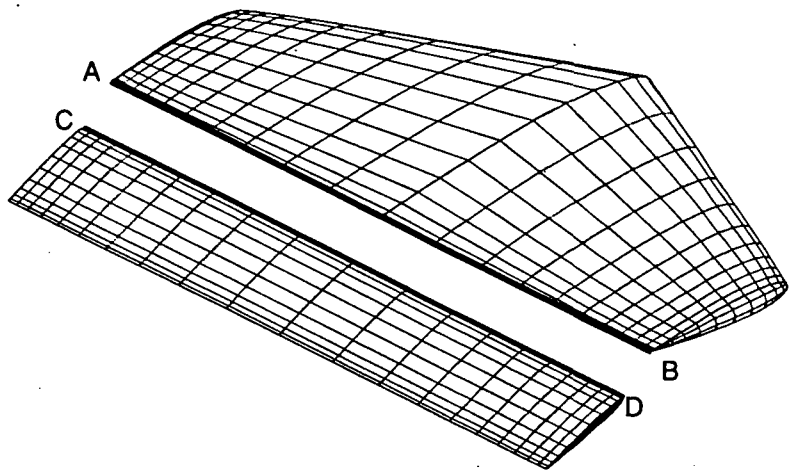

Fig. 5 A generic high-lift configuration wing and bridging edges (A-B and C-D)

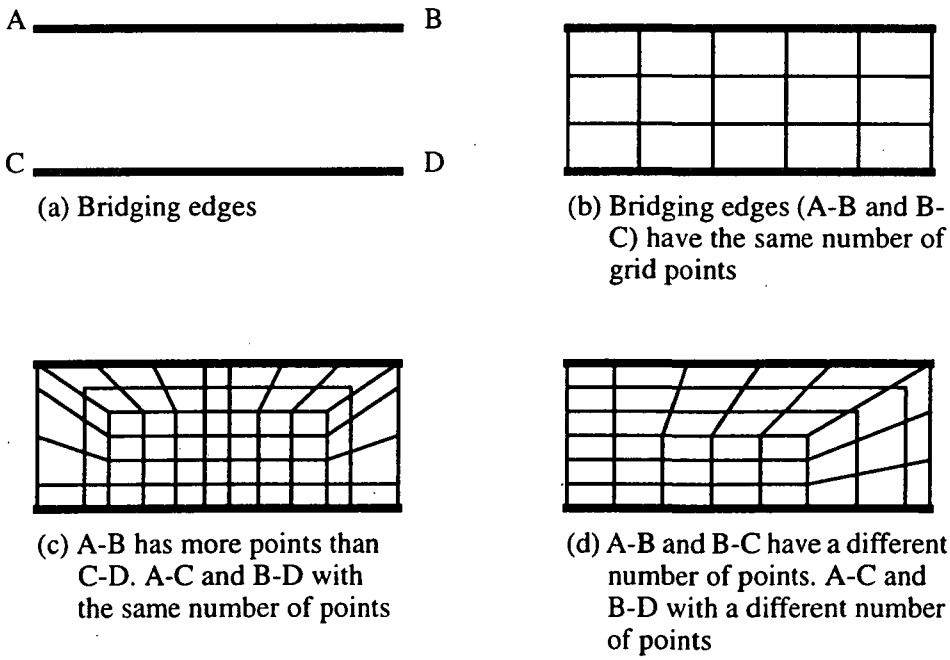

(a) Bridging edges

(b) Bridging edges (A-B and B-C) have the same number of grid points

(c) A-B has more points than C-D. A-C and B-D with the same number of points

(d) A-B and B-C have a different number of points. A-C and B-D with a different number of points

Fig. 6 Formation of "bridging" fronts

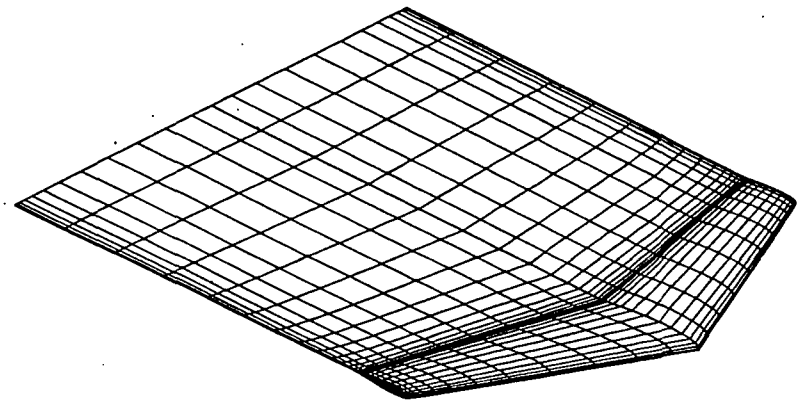

(a) Single initial front (body surface and wake plane)

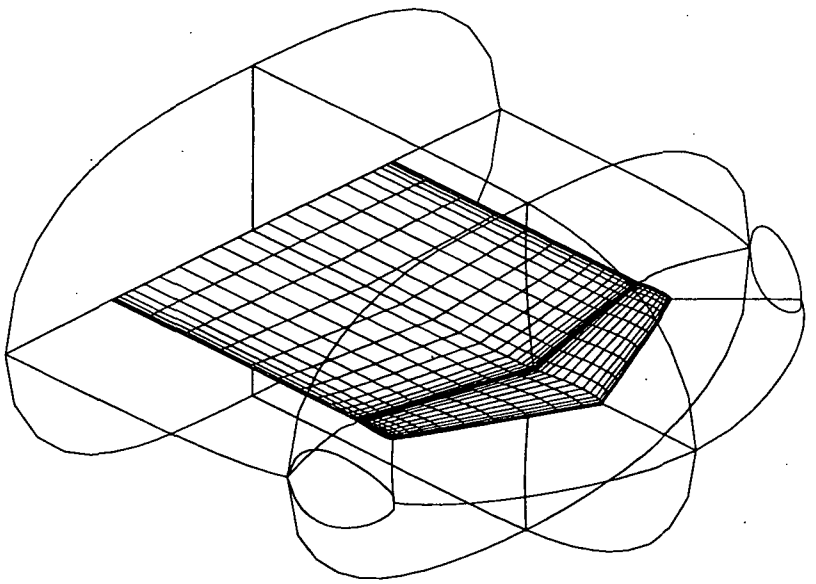

(b) Block edges of the resulting 6 block volume grid together with the boundary grid lines along the symmetry plane

Fig. 7 Grid generation for a single swept-back wing with a single initial front

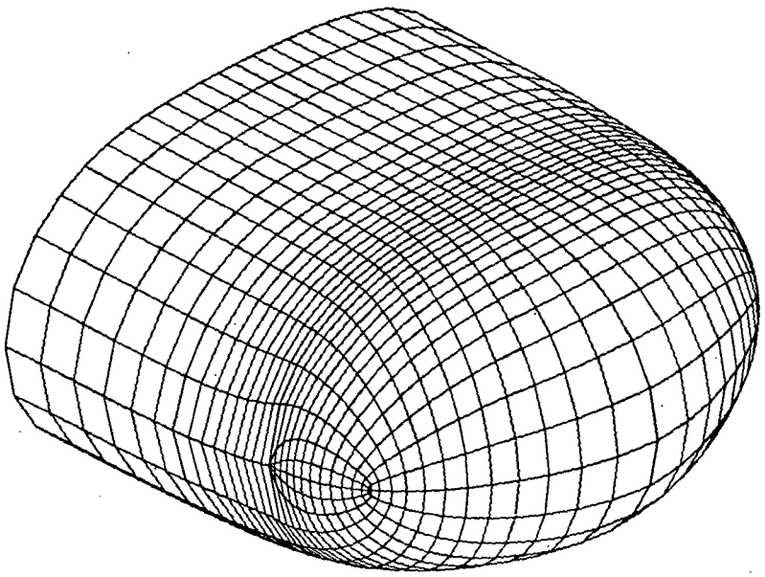

(c) Outer block boundaries

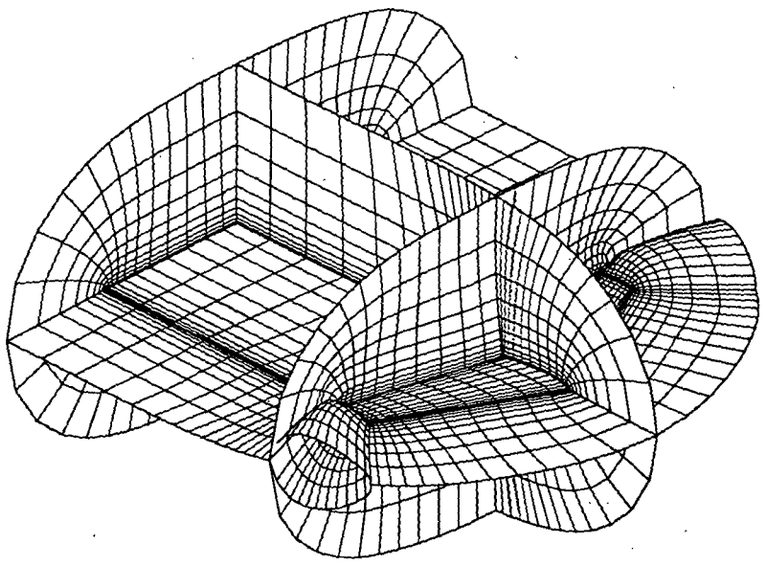

(d) Internal block boundaries and the symmetry plane

Fig. 7 (Continued) Grid generation for a single swept-back wing with a single initial front

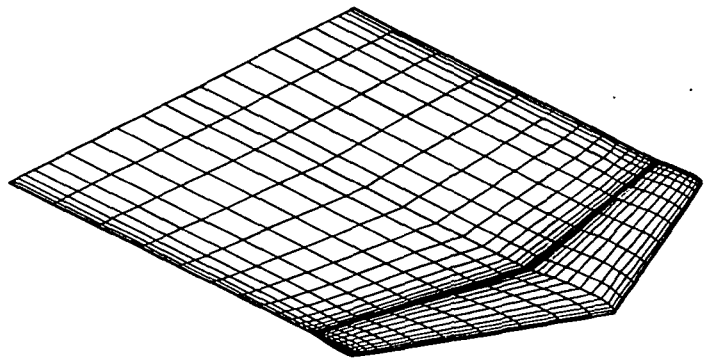

(a) 3 initial fronts (body surface and wake plane)

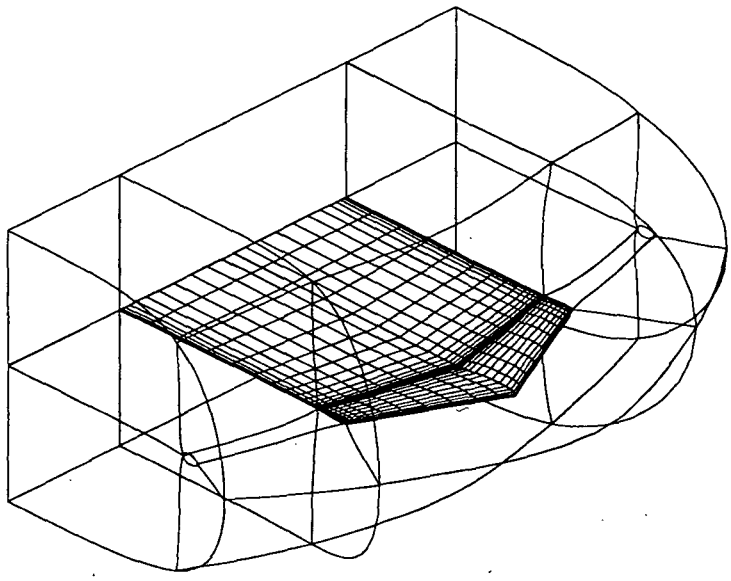

(b) Block edges of the resulting 14 block volume grid

Fig. 8 Grid generation for a single swept-back wing with 3 initial fronts

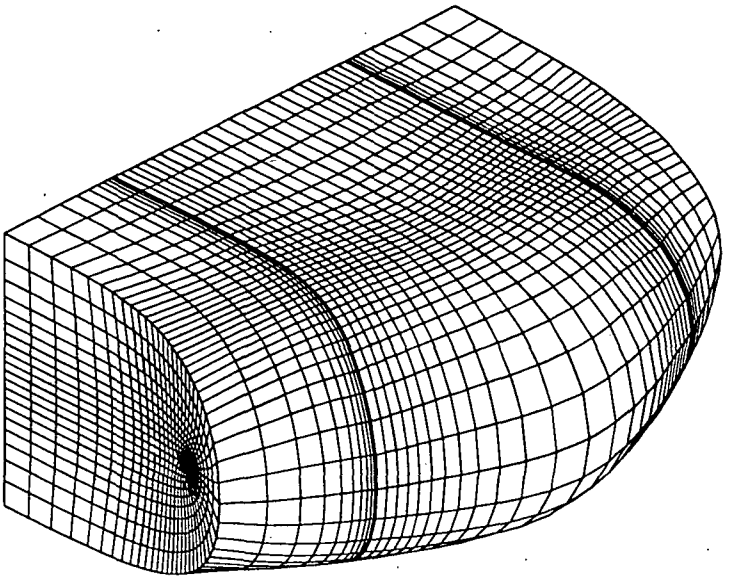

(c) Outer block boundaries

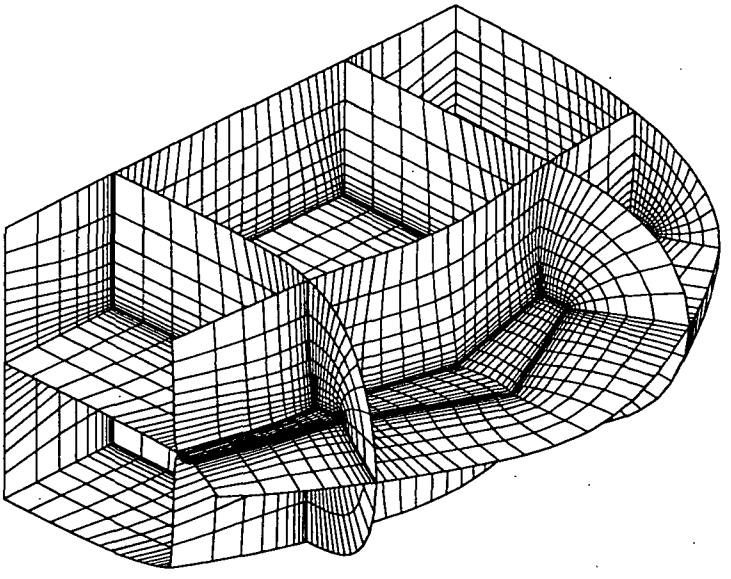

(d) Internal block boundaries

Fig. 8 (Continued) Grid generation for a single swept-back wing with 3 initial fronts

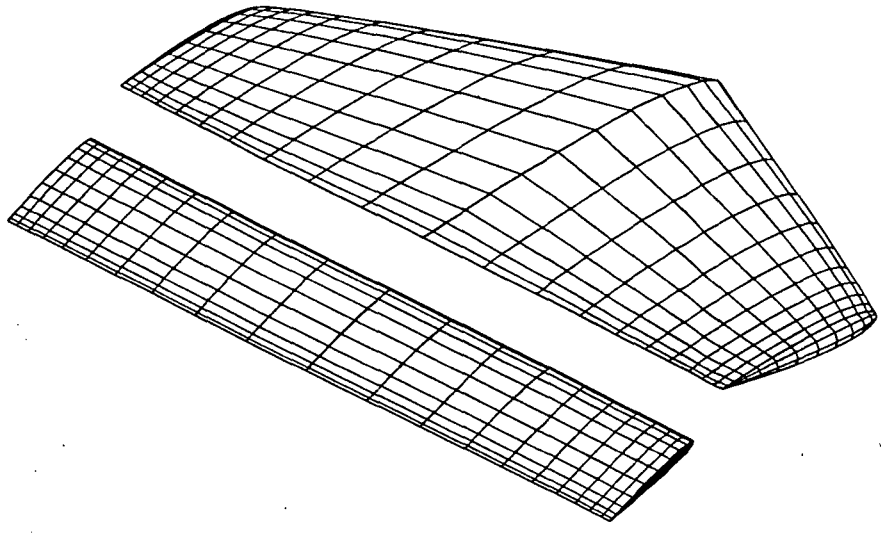

(a) Initial fronts (main wing and flap)

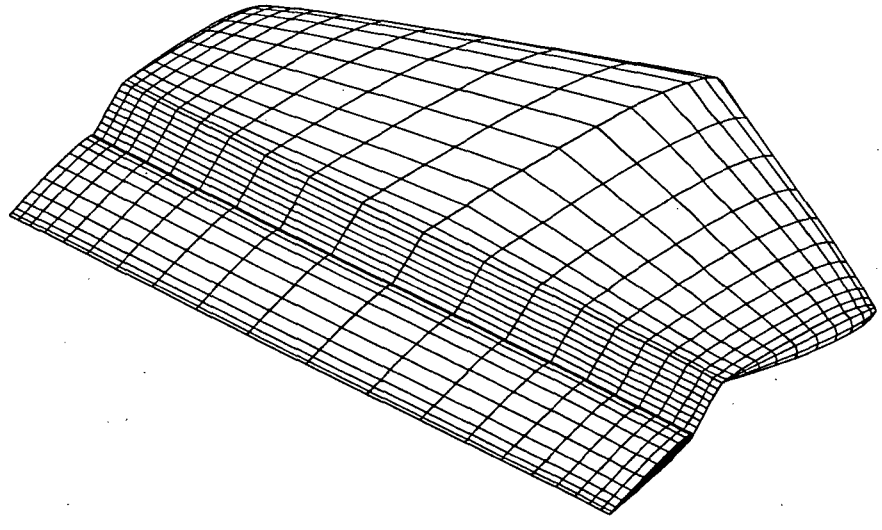

(b) Gap between the main wing and the flap is filled with a "bridging" front

Fig. 9 Grid generation for a generic high-lift configuration (28 block volume grid)

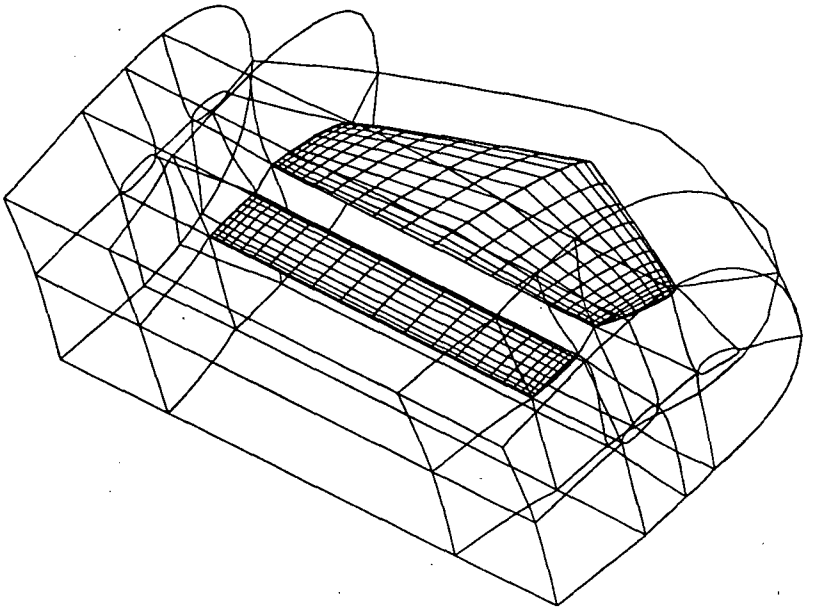

(c) Block edges of the resulting volume grid

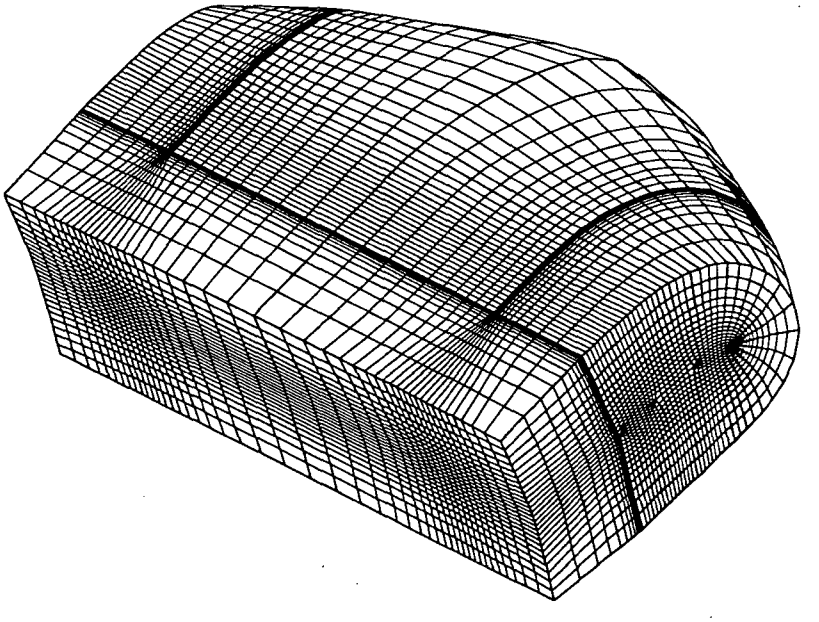

(d) Outer block boundaries

Fig. 9 (Continued) Grid generation for a generic high-lift configuration (28 block volume grid)

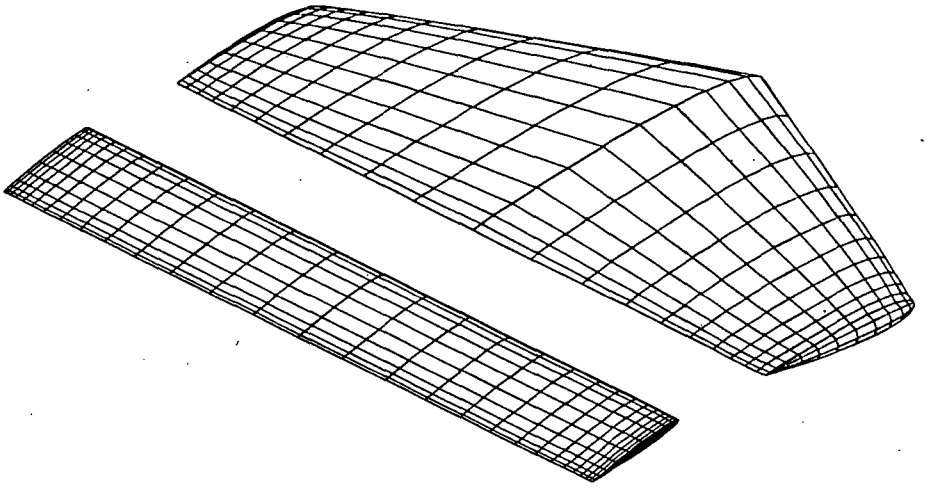

(a) Initial fronts (main wing and flap)

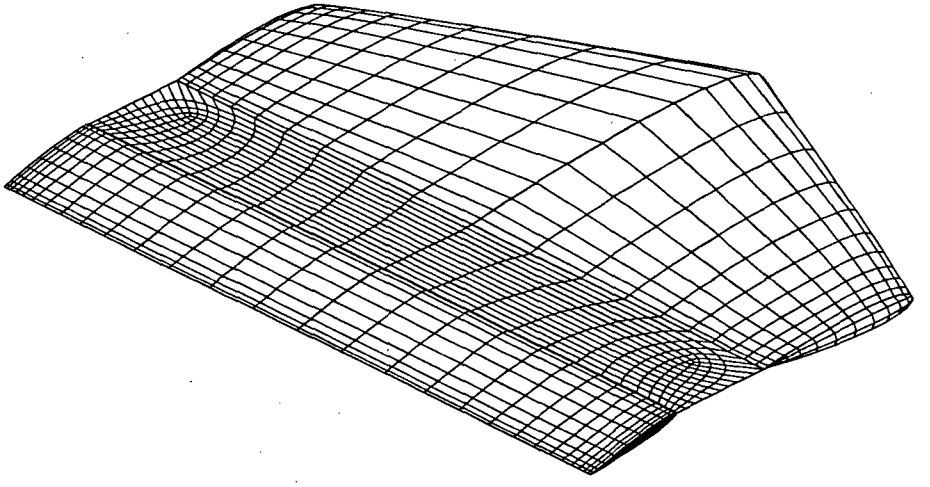

(b) Gap between the main wing and the flap is filled with a "bridging" front

Fig. 10 Grid generation for a generic high-lift configuration (38 block volume grid)

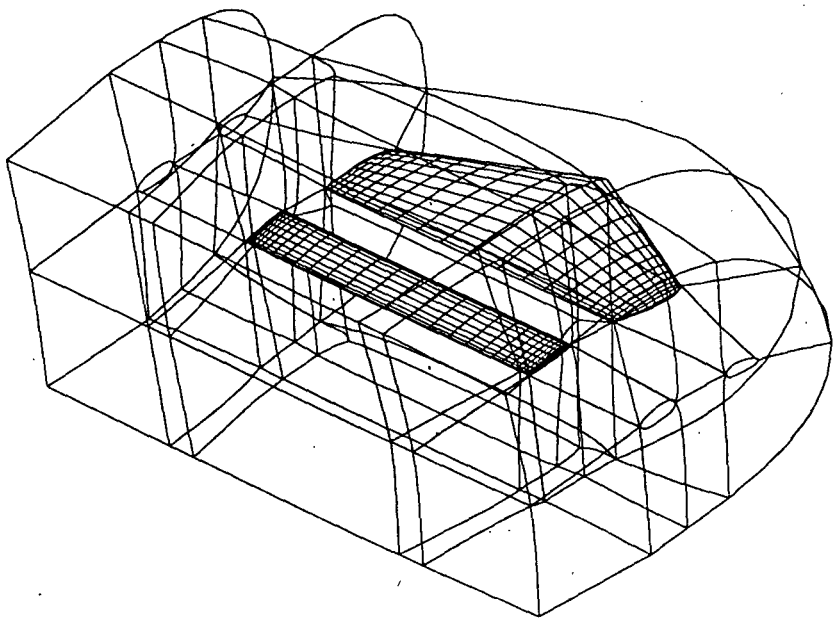

(c) Block edges of the resulting volume grid

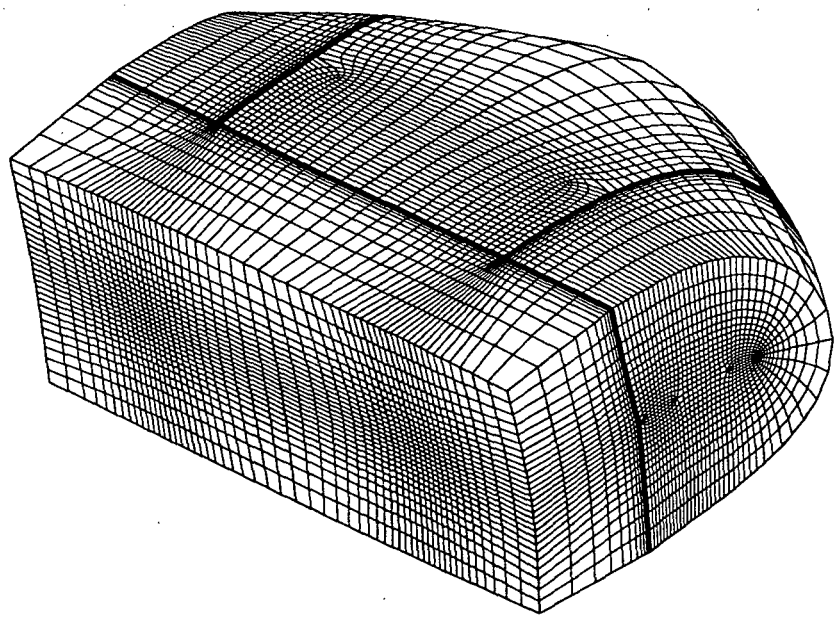

(d) Outer block boundaries

Fig. 10 (Continued) Grid generation for a generic high-lift configuration (38 block volume grid)